Polisztirolbetonba ágyazott hidegen alakított acél viselkedésének numerikus vizsgálata külpontos nyomás esetén

Numerical investigations on polystyrene aggregate concrete encased cold formed steel elements subjected to eccentric compression

ALABEDI Ahmed [1*]***, Dr. HEGYI Péter*** [1]

[1]Department of Structural Engineering, Budapest University of Technology and Economics,
Műegyetem rkp. 3, 1111 Budapest,Hungary
* Corresponding author, e-mail: alabedi.ahmed@edu.bme.hu

Abstract

This paper investigates the structural behaviour of polystyrene aggregate concrete encased cold-formed steel sections subjected to eccentric compression through detailed finite element modelling. A comprehensive parametric study was conducted to evaluate the effect of different parameters on the load-bearing capacity, such as load eccentricity, core steel thickness, and yield strength. As a result, a predictive equation was derived based on FEM outcomes to estimate load reduction compared to a centric case based on normalized load eccentricity.

Keywords: cold-formed steel, polystyrene aggregate concrete (PAC), eccentric compression, FEM, axial-bending interaction

Kivonat

A cikk a polisztirol adalékos betonba burkolt, hidegen alakított acélszelvények külpontos nyomás hatására bekövetkező szerkezeti viselkedését vizsgálja fejlett végeselem-modell segítségével. Átfogó paramétervizsgálatot végeztünk annak érdekében, hogy értékeljük a különböző tényezők – például a teher külpontossága, az acél vastagsága és a folyáshatár – hatását a teherbírásra. Ennek eredményeként a modell eredményei alapján egy közelítő egyenlet került meghatározásra, amely a normalizált teher külpontossága alapján becsli a teherbírás központos esethez képesti csökkenését.

Kulcsszavak: hidegen alakított acél, polisztirolbeton, külpontos nyomás, végeselem-módszer, nyomás–hajlítás interakció

1. INTRODUCTION

Sustainable structures have gained wide attention in modern constructions as they reduce environmental impact and save resources. In this field, the Budapest University of Technology and Economics hosted a new project of encased cold-formed steel (CFS) in which polystyrene aggregate concrete (PAC) was utilised as encasing material, providing a continuous bracing effect [1]. The new complex structure is distinguished by its cost-efficiency and sustainability impact. From the definition, PAC has no gravel or sand and may even utilize waste polystyrene, reducing environmental pollution and leading to reduced material use and energy consumption in transportation and construction. Besides, its excellent thermal insulation properties contribute to energy-efficient buildings [2]. Conversely, CFS is a cost-effective structure characterised by light section weight, speed of production, and ease of manufacturing process.

The main goal of the research project was to understand the impact of encasing material on the behaviour of CFS and utilise the experimental outcomes in developing a Eurocode-based design procedure. In [3–6], an extensive experimental program was carried out in which encased CFS was tested under varying load conditions, tension, compression, shear, and eccentric loading. In the first series [3,4], encased beams and columns were deeply investigated to gain information on the new complex element loading capacity and failure

phenomena. The test results demonstrated the beneficial impact of PAC on the stability of tested elements, in which load-bearing capacity increased by 10-190% compared to pure steel ones. The test results revealed the superior impact of PAC on restraining global and distortional buckling and consequently increasing load-bearing capacity. Moreover, shear tests were also investigated on wall panels [4,6], and the test results were found to be consistent with previous findings in which all tested panels failed locally. End joints were also deeply investigated for a more efficient building system. In [5], sixth-end connection types and four steel cross-sections were examined. The experimental findings emphasised that the end connection is a key parameter influencing the overall structural behaviour of the detail.

Apart from experiments, the new complex system was numerically evaluated on different levels. In [1], a PAC-encased steel plate was numerically modelled to assess the newly presented design method. Moreover, a fully encased C-section was also investigated in [7,8]. However, the complexity of new elements led to their finite element (FE) modelling being more problematic and time-consuming. Hence, Eid et al. introduced a new modelling technique by replacing the PAC block with a one-directional equivalent spring similar to the Winkler foundation [7]. Later, the performance of the simplified model was deeply investigated and enhanced by the authors, making the simplified model a universal tool that can be used efficiently for calculating the resistance of any elastic material encased CFS section [8,9].

In 2024, the behaviour of encased CFS was investigated by considering different load types, i.e., eccentric compression [10]. The main experimental goal is to expand the range of results and deeply investigate the impact of applied bending moment on PAC enhancement, besides utilizing experimental outcomes in developing new design procedures that account for axial bending interaction. In this paper, the effect of the eccentric load is numerically investigated. The final aim is to expand the available experimental results and investigate the impact of different parameters on overall section resistance. Eventually, as there is no available design for eccentrically loaded encased C-section, a closed-form equation can be derived based on numerical model results that can be used directly to estimate the reduction in load for a given loading case.

2. EXPERIMENTAL TESTS

The previously conducted experiments on PAC-encased cold-formed steel (CFS) primarily focused on a single loading type. As a result, experimental data on PAC-encased CFS subjected to eccentric compression remain limited. The only available studies were carried out by the authors and are reported in [10]. A total of fourteen encased CFS specimens were tested under three distinct loading conditions. The tested sections consisted of C-profiles with a 150 mm web height and were made of S350GD steel grade. Each specimen was 300 mm in length and fully embedded in a 300 × 300 mm polystyrene aggregate concrete (PAC) block (see Figure 1). To improve load transfer, a web-stiffened end-joint configuration was adopted based on recommendations from previous studies. Each C-section was connected to a 300 mm long U-section to provide a stable loading surface. Additionally, 50 × 50 mm steel angles were installed along the web of the C-section to enhance stiffness and shift the failure away from the connection zone toward the column itself [5].

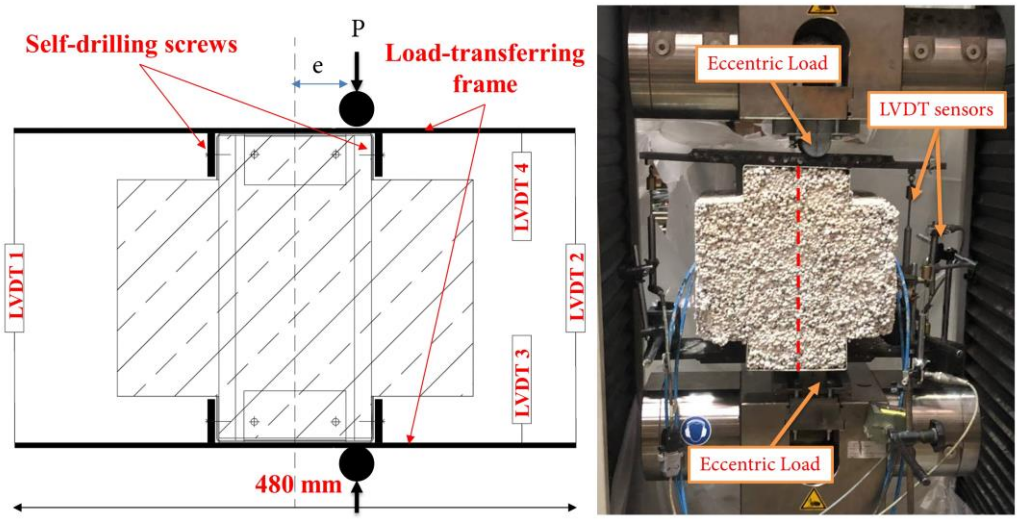

Fig.1 Tested setup [10]

Eccentric loading was applied through a 20 mm thick hot-rolled steel frame attached to both ends of the specimen, using self-drilling screws to ensure proper load transfer. The tests were displacement-controlled, and the load was applied on the outer surface of the loading frame at various eccentricities measured from the centroid of the gross cross-section. This load shifting introduced bending moments about the strong axis, resulting in axial-bending interaction. The experimental results showed that local buckling dominated the failure mode, with the failure zone shifting toward the loaded side of the section. The total reduction in load-bearing capacity, compared to the centric resistance, ranged between 20% and 52%, influenced by the load position and the thickness of the core steel.

3. NUMERICAL MODEL DEVELOPMENT

An advanced finite element (FE) model was developed using ANSYS Mechanical APDL, employing the four-node SHELL181 element to replicate the experimental tests. The steel material properties were defined using a bilinear stress-strain curve with isotropic hardening, with an elastic modulus of 210 GPa and a Poisson's ratio of 0.3. Actual material properties and thicknesses, as provided in Table 1, were used. Two types of contact elements were implemented to simulate the contact surfaces. For line-to-surface contact, CONTACT177 and TARGET170 elements were used to model the interaction between the top edge of the C-section and the upper web of the U-section. All remaining contact areas were modelled using surface-to-surface contact through CONTACT174 and TARGET170 elements.

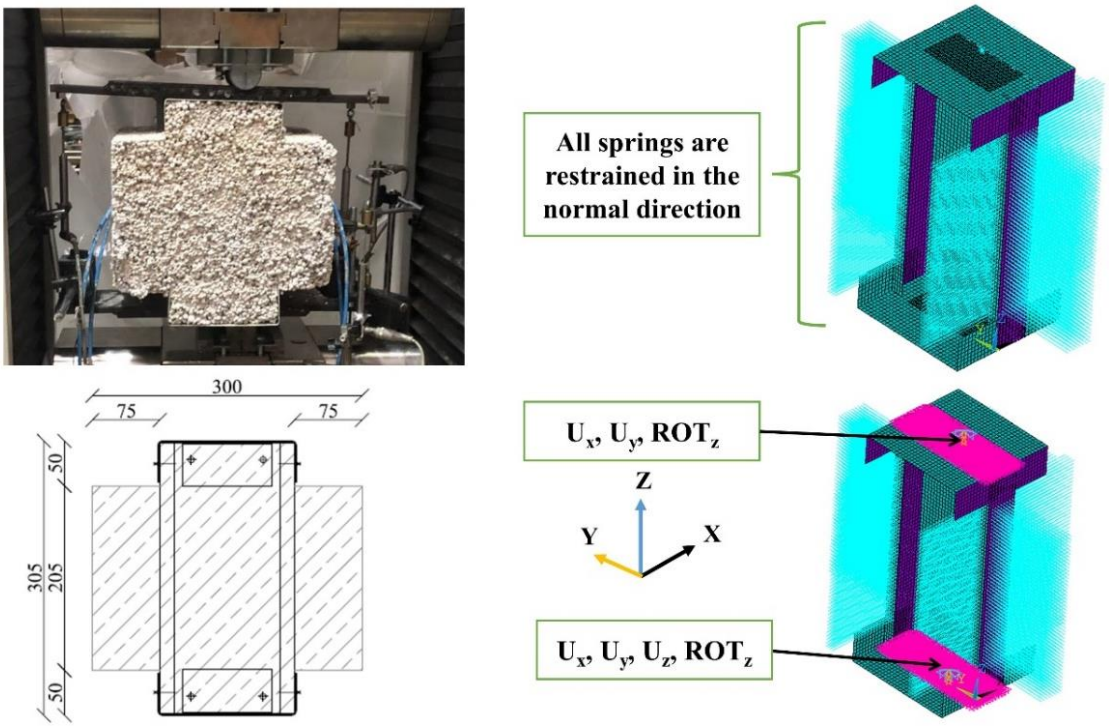

Fig. 2 3D model illustration and boundary conditions

Rigid node-to-node links were applied to represent the connecting screws, while spot welding between the L and the web of the U sections was modeled using the six-degree-of-freedom COMBIN40 element. For the encasing material, a simplified modelling approach based on references [8,9] was adopted. PAC was replaced with unidirectional COMBIN40 springs of equivalent stiffness. The elastic modulus of concrete was set to 50 MPa, reflecting an average value due to the high variability in the properties of PAC material compared to conventional materials [1]. A mesh sensitivity analysis determined the optimal element size (v). A mesh size of 5 mm was found to deliver accurate results; however, a finer mesh of size v/2 was applied to the top and bottom L-sections to improve contact performance. The boundary conditions are shown in Figure 2, where two master nodes were utilised to connect the surface nodes of the U-section. Additionally, all COMBIN40 springs were constrained in the normal direction. A geometrically and materially nonlinear (GMNI) analysis was performed, accounting for both material nonlinearity and geometric imperfections. Geometric imperfections were introduced as the lowest eigenmode shape, scaled by factors of b/200 for internal plates and b/50 for outstanding plates.

4. EVALUATION OF RESULTS

The finite element (FE) model was first validated through a geometrically and materially nonlinear (GMNI) analysis to determine the ultimate strength, following the simplified modelling procedure described in [8,9]. The FE results demonstrated strong agreement with experimental data, exhibiting an average error of approximately 5%. In all FE simulations, local buckling was identified as the governing failure mode. Table 1 and Figure 3 illustrate the comparison between FE model resistance and observed failure modes from the experiments. Consequently, the end-joint configuration was excluded, and a parametric study was performed to examine the effect of load eccentricity, as end joints can influence results. Moreover, this study analyzed five different commercially available C-sections with varying web heights, namely C90, C100, C120, C140, and C150, of different core steel thicknesses from 0.9 mm to 2 mm, covering a wide range of steel yield strengths.

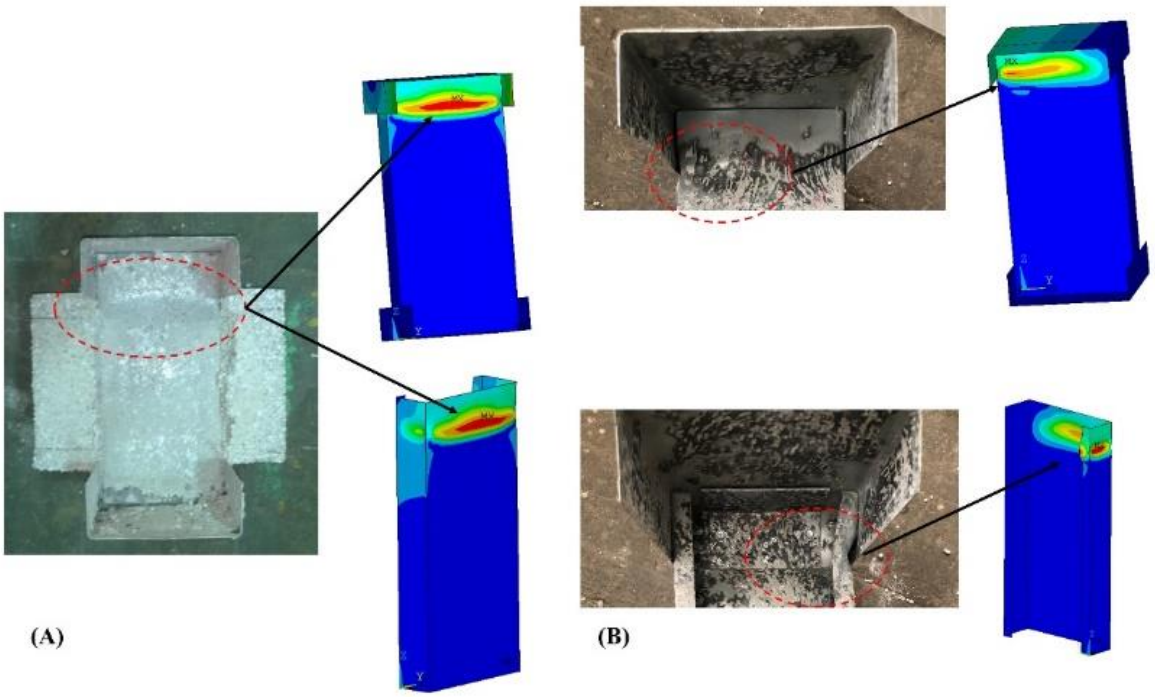

Fig. 3 Failure mode comparison of FEM: A) C150-10-300-E0, B) C150-10-300-E1

FEM results vs experiments Table 1.

#	fy [MPa]	Eccentricity [mm]	R_{test} [kN]	R_{FEM} [kN]	R_{FEM}/R_{test}-1
C150-10-300-E0	322	0	42.03	43.4	0.03
C150-10-300-E1	370	37.5	33.67	35.70	0.06
C150-10-300-E2		50	28.88	30.50	0.06
C150-10-300-E3		75	22.94	24.30	0.06
C150-20-300-E1	405	0	130.27	137.65	0.06
C150-20-300-E1	429	37.5	109.74	114.9	0.05
C150-20-300-E2		50	86.5	90.15	0.04

5. PARAMETRIC STUDY

The parametric study evaluated six levels of load eccentricity, as illustrated in Figure 4. The percentage reduction in load-bearing capacity was plotted as a function of applied eccentricity. Two distinct behavioural phases were identified. The reduction rate increased rapidly in the first phase up to e=h/4, while beyond h/4, the rate of reduction continued but at a slower rate across all sections. Overall, load reduction was found to be nearly proportional to the applied eccentricity, ranging from approximately 16% at e=h/8 to 57% at e=2h/3. The influence of core steel thickness was also examined. Figure 5 compares the reduction curves for sections with two different core steel thicknesses. The results indicate that section thickness affects the overall performance of PAC. As reported in [10], increasing steel thickness enhances the stiffness of the steel core, reducing the contribution of PAC. Further explanation, Eq.1 showed that the b/t ratio highly influences the critical buckling stress of the encased plate. A higher b/t leads to a higher partial slenderness ratio, which increases the reduction factor and decreases the effective section modulus (W_{eff}). Across the range studied, the impact of core steel thickness was found to be limited, with variations between 2% and 4%.

$$\sigma_{cr,p} = 4\frac{\pi^2 E_s}{12(1-v_s^2)(b/t)^2} - \frac{4680MPa}{b/t} + 2.35E_c + \sqrt{E_c 3025MPa} \quad (1)$$

Similarly, the effect of steel yield strength was assessed. Figure 6 presents reduction curves for different C-sections with varying yield strengths (fy). The results revealed that increasing fy had a minimal effect on reducing the load reduction percentage, with differences ranging from 3% to 4%. This limited effect is attributed to the increased partial slenderness ratio at higher yield strengths, which leads to higher reduction factors and reduced Weff. Consequently, the amount of enhancement is limited, as the ultimate moment capacity (Mrd) is defined by W_{eff}*fy.

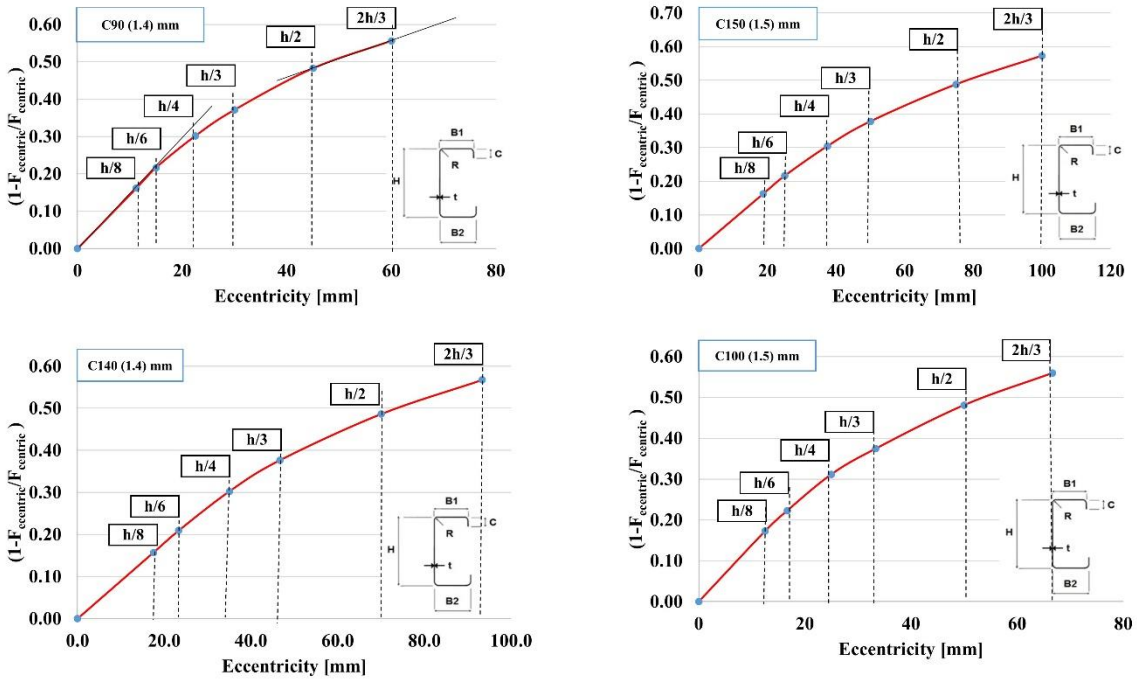

Fig. 4 Reduction curves of different C-sections

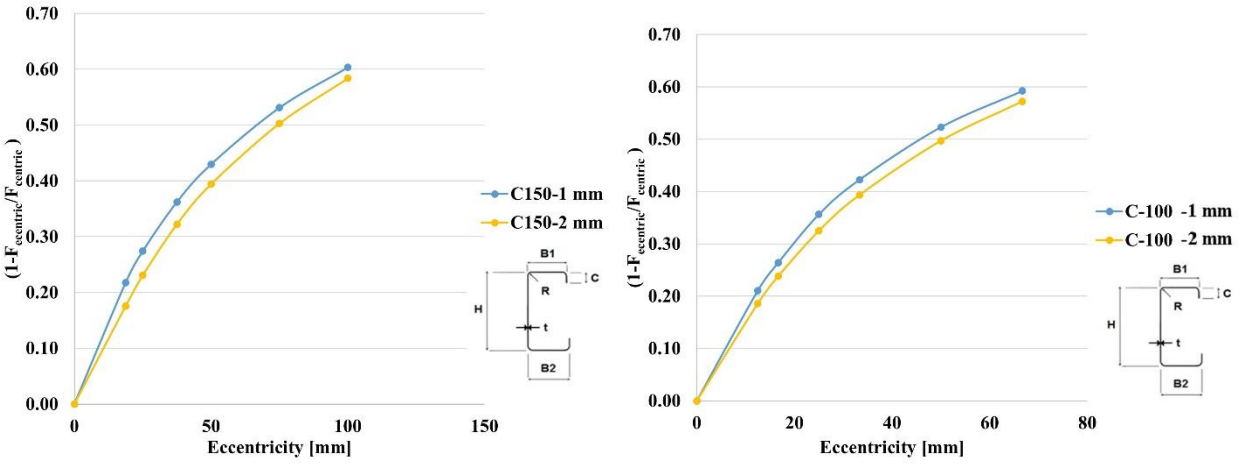

Fig. 5 Core steel impact

In conclusion, the parametric study showed that load reduction is primarily governed by the percentage of load shifting relative to the web height of the section. Among all parameters investigated, load eccentricity showed the most significant impact on reduction behaviour and can be reliably used to estimate load reduction. Figure 7 displays four reduction curves for different C-sections, with applied eccentricity normalised to the corresponding web heights.

$$R = 0.71\left(1 - \ exp^{-2.56\frac{e}{h_w}}\right) \tag{2}$$

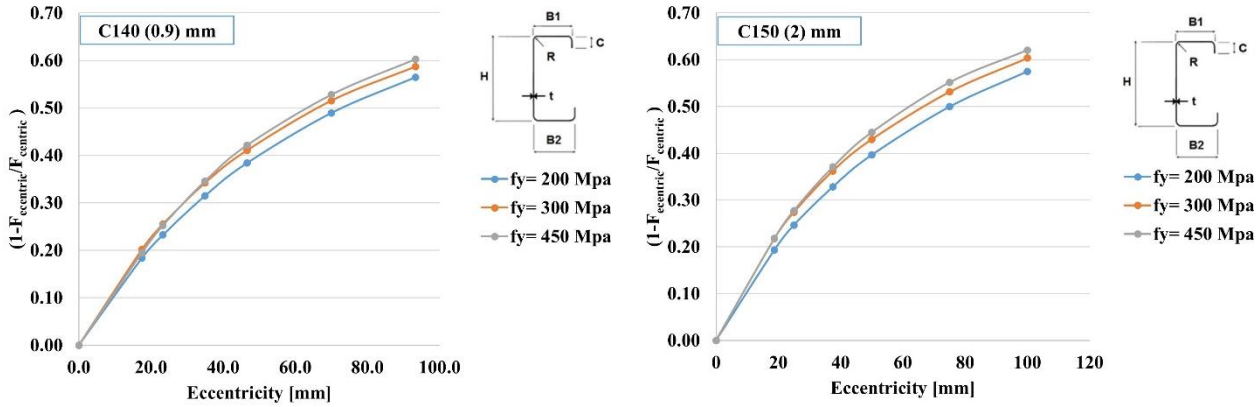

Fig. 6 Steel yield strength effect on load reduction

The variation among these curves was found to be limited to 3%. Based on these findings, a numerical tool was employed to derive Eq. 2, which estimates the reduction percentage as a function of section height. This equation can be directly applied with the detailed design method outlined in [1] to evaluate the load-bearing capacity under eccentric loading conditions. However, it should be noted that the applicability of Equation 2 is limited to the scope of this study. Where R is the reduction percentage, e [mm] is the applied eccentricity, and h_w [mm] is the section web height.

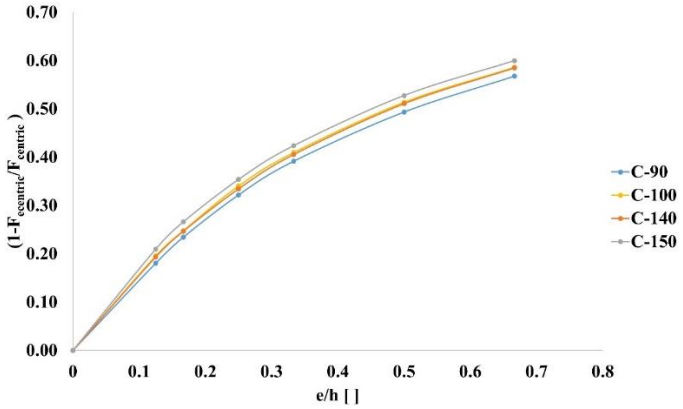

Fig. 7 Load reduction curves as a function of normalised eccentricity

CONCLUSION

This study delivered a comprehensive numerical investigation of the behaviour of PAC-encased cold-formed steel sections under eccentric compression. The developed finite element model strongly agreed with experimental results, accurately capturing local buckling as the dominant failure mode. A detailed parametric study was conducted, and the results revealed that load eccentricity has the most significant influence on the load-bearing capacity, with reductions ranging from 16% to 57% depending on the level of eccentricity. In contrast, core steel thickness and yield strength showed only minor effects. Eventually, load reduction was found to correlate strongly with the normalised load-shifting distance relative to web height. Based on this relationship, a predictive equation was derived to estimate load reduction percentage, offering a direct way that can be used for future design considerations within the defined range.

REFERNCES

[1] A. Alabedi, P. Hegyi, *Development of a Eurocode-based design method for local and distortional buckling for cold-formed C-sections encased in ultra-lightweight concrete under compression*, Thin-Walled Structures 196 (2024) 111504. https://doi.org/10.1016/j.tws.2023.111504.

[2] É. Lublóy, L.G. Balázs, K. Kopecskó, E. Tóth, L. Dunai, P. Hegyi, O. Drávucz, *Thermal insulation capacity of concretes by expanded polystyrene aggregate*, in: The Fourth International FIB Congress, 2014: pp. 750–751.

[3] P. Hegyi, L. Dunai, *Experimental investigations on ultra-lightweight-concrete encased cold-formed steel structures: Part II: Stability behaviour of elements subjected to compression*, Thin-Walled Structures 101 (2016) 100–108. https://doi.org/10.1016/j.tws.2016.01.003.

[4] P. Hegyi, L. Dunai, *Experimental study on ultra-lightweight-concrete encased cold-formed steel structures Part I: Stability behaviour of elements subjected to bending*, Thin-Walled Structures 101 (2016) 75–84. https://doi.org/10.1016/j.tws.2016.01.004.

[5] P. Hegyi, L. Dunai, *Experimental Investigation of Thin-walled Column-end Joints Encased in Ultra-lightweight Concrete*, Periodica Polytechnica Civil Engineering 61 (2017) 951–957. https://doi.org/https://doi.org/10.3311/PPci.10041.

[6] P. Hegyi, L. Horváth, L. Dunai, A.A.M. Ghazi, *Experimental Investigation of Shear Effects in Ultra-Lightweight Concrete Encased CFS Structural Members*, Ce/Papers 5 (2022) 143–150. https://doi.org/https://doi.org/10.1002/cepa.1739.

[7] N. Eid, A.L. Joo, *Simplified numerical model development for advanced design of lightweight-concrete encased cold-formed steel compressed elements*, Advances in Civil Engineering 2022 (2022).

[8] A. Alabedi, P. Hegyi, *Assessing the equivalent spring modelling method of CFS elements encased in ultra-lightweight concrete*, Bulletin of the Polish Academy of Sciences Technical Sciences (2024) 151384–151384. https://doi.org/10.24425/bpasts.2024.151384.

[9] A. Alabedi, P. Hegyi, *Assessing the Equivalent Spring Method for Modelling of Lightweight-concrete Encased Cold-formed Steel Elements in Compression*, Periodica Polytechnica Civil Engineering 68 (2023) 305–313. https://doi.org/10.3311/PPci.22803.

[10] A. Alabedi, P. Hegyi, *Experimental investigations on ultralightweight-concrete encased cold-formed steel structures: Local stability behaviour of Csection profiles subjected to eccentric compression*, Bulletin of the Polish Academy of Sciences Technical Sciences (2024) 151044–151044. https://doi.org/10.24425/bpasts.2024.151044.